The geometry and phase transition behavior of configuration mixing in the interacting boson model

P. Van Isacker
Grand Accélérateur National d'Ions Lourds,
BP 55027, F-14076 Caen Cedex 5, France

I. Morales
Instituto de Ciencias Nucleares, UNAM,
Apartado Postal 70-543, 04510 México, D.F. Mexico.

C.E. Vargas
Facultad de Física e Inteligencia Artificial, UV, Sebastián Camacho;
Centro, Xalapa, Ver., 91000, Mexico

A. Frank
Instituto de Ciencias Nucleares, UNAM,
Apartado Postal 70-543, 04510 México, D.F. Mexico.

Recibido el 5 de febrero de 2005; aceptado el 20 de marzo de 2005

The Interacting Boson Model (IBM) with configuration mixing can be given a geometrical interpretation, when used in conjunction with a (matrix) coherent-state method. This approach can be used to study the geometric aspects of shape coexistence in nuclei, as well as the phase space diagrams associated to this phenomenon.

Keywords: Algebraic models; shape coexistence; phase transition; Configuration Mixing.

Se muestra que es posible hacer una interpretacion geometrica del modelo de bosones interactuantes (IBA) al utilizar la mezcla de configuraciones junto con el metodo de la matriz de estados coherentes. Esta aproximacion puede utilizarse para estudiar los aspectos geometricos de la coexistencia de forma en el nucleo, asi como los diagramas de fase asociados a este fenomeno.

Descriptores: Modelos algebraicos; coexistencia de forma, transición de fase; Mezcla de configuraciones.

PACS: 21.10.Re; 21.60.Ev; 21.60.Fw; 27.70.+q

1. Shape coexistence in Nuclei

In the last 20 years there has been much interest in the study of nuclear coexistence phenomena, understood as the possibility of a simultaneous excitation of nuclear configurations which may lead to shape phase transitions [1].

The structural changes in the properties of physical systems are called phase transitions. These changes have long been studied in systems such as water in its gaseous, liquid and solid forms, the so-called thermodynamic phase transitions, where the control parameter is the temperature T.

Phase transitions may occur as some of the control parameters that constrain the system are varied. In the late 70's, Gilmore et al. [2] introduced phase transitions in which the control parameter g, is a parameter appearing in the quantum Hamiltonian describing the system. These "ground state energy phase transitions", are in some ways similar to thermodynamic phase transitions and are known today as "quantum phase transitions".

In the context of the nuclear shell model the origin of coexistence can be traced back to many-particle many-hole excitations across shell gaps, which become energetically favourable as a result of the interplay between shell effects and the neutron-proton interaction [3]. For example, in the neutron-deficient lead isotopes, shape coexistence was predicted by May *et al.* [4] in a Nilsson framework including shell corrections.

Subsequent deformed mean-field calculations have predicted the occurrence in the energy surface of close-lying oblate and prolate minima near the ground-state spherical configuration, specifically in lead nuclei with neutron number close to $N = 104$ (see, *e.g.*, Ref. 5). These predictions have been confirmed by a series of experiments on the neutron-deficient lead isotopes, culminating in the recent observation of three close low-lying 0^+ levels in ^{186}Pb [6], interpreted as having spherical, oblate, and prolate shapes. In Fig. 1 is shown the systematics of the 0^+ states in the lead chain. Present-day sophisticated mean-field calculations [7] can account for these three minima in a region of energy that is consistent with experimental findings. Although these theoretical studies are very impressive, they have focussed mainly on the properties of the potential energy surface of ^{186}Pb. A

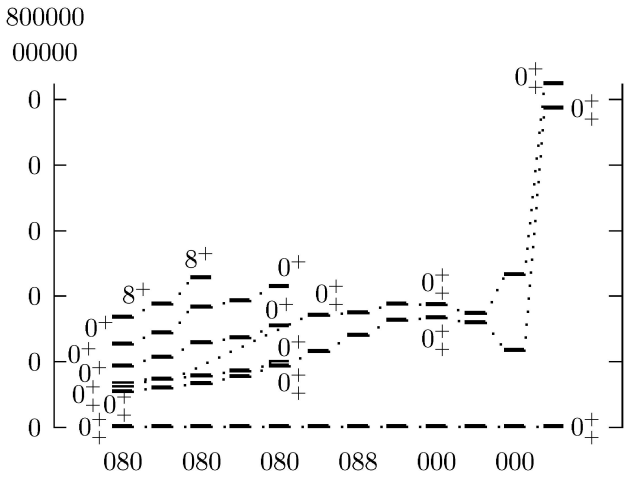

FIGURE 1. Systematics of low-lying 0^+ states in ^{186}Pb.

description beyond mean field that includes spectroscopic properties requires simplifying assumptions such as axial symmetry and even then it represents a major computational effort. Shell-model calculations, on the other hand, are very difficult to carry out in this region due to the rapidly increasing size of the model space, particularly for the case of interest, which involves the opening up of shells through particle-hole (p-h) configurations.

The Interacting Boson Model (IBM) [8] provides a simple alternative to describe the phenomenon of nuclear coexistence. The model assumes that low-lying collective excitations of the nucleus can be described in terms of the number N of s and d bosons. The bosons correspond to pairs of nucleons in the valence shell, coupled to angular momentum 0 or 2; N is constant for a given nucleus and equal to half its number of valence nucleons. Core (*i.e.*, non-valence p-h) excitations can be included in a natural way since they correspond to configurations with higher numbers of active nucleons and thus with higher boson numbers. Specifically, 0p-0h, 2p-2h, 4p-4h, ... shell-model configurations correspond to systems of N, $N+2$, $N+4$, ... interacting bosons which are simultaneously treated and possibly mixed in this configuration-mixed version of the IBM [9]. This model was applied recently to describe the evolving properties of the lead isotopes [10].

While both mean-field theory and IBM give a satisfactory description of nuclear coexistence, an obvious connection between them is lacking. In this contribution we argue that the algebraic description of nuclear coexistence can be given a geometric interpretation and hence be connected with mean-field theory [11]. This approach opens the possibility for a study of the relation between coexistence and criticality.

2. The IBM with configuration mixing

We first explain the essential ingredients of the model with specific reference to the lead isotopes. The model space for three configurations is built from N, $N+2$, and $N+4$ bosons and constitutes a boson representation of the shell-model configurations that are dominant in the low-energy region of the lead isotopes. The N-boson states correspond to excitations of neutrons only, for which the proton shell $Z = 82$ remains closed; they can be characterized as the 0p-0h configuration. The states with $N+2$ and $N+4$ bosons correspond to 2p-2h and 4p-4h excitations of the protons across the $Z = 82$ shell gap coupled the valence neutrons in the $N = 82$-126 shell. The Hamiltonian is

$$\hat{H} = \hat{H}_{0\mathrm{p}-0\mathrm{h}} + \hat{H}_{2\mathrm{p}-2\mathrm{h}} + \hat{H}_{4\mathrm{p}-4\mathrm{h}} + \hat{H}^{02}_{\mathrm{mix}} + \hat{H}^{24}_{\mathrm{mix}}, \quad (1)$$

where $\hat{H}_{i\mathrm{p}-i\mathrm{h}}$ is the Hamiltonian for the ith of the three configurations, taken in the simplified form [12]

$$\hat{H}_{i\mathrm{p}-i\mathrm{h}} = \epsilon_i \hat{n}_d + \kappa_i \hat{Q}_i \cdot \hat{Q}_i. \quad (2)$$

This Hamiltonian provides a simple parametrization of the essential features of nuclear structural evolution in terms of a vibrational term $\hat{n}_d$ (the number of d bosons) and a quadrupole interaction $\hat{Q}_i \cdot \hat{Q}_i$ with $\hat{Q}_i = (s^\dagger \tilde{d} + d^\dagger s)^{(2)} + \chi_i (d^\dagger \tilde{d})^{(2)}$. The Hamiltonian (2) conserves the number of bosons and does not provide any mixing between the N, $N+2$, and $N+4$ configurations. Configuration mixing arises through the boson-number non-conserving parts $\hat{H}^{ii'}_{\mathrm{mix}}$ which are assumed to have the simple form [9]

$$\hat{H}^{ii'}_{\mathrm{mix}} = \omega_0^{ii'} (s^\dagger s^\dagger + ss) + \omega_2^{ii'} (d^\dagger \cdot d^\dagger + \tilde{d} \cdot \tilde{d}), \quad (3)$$

with $ii' = 02$ or 24. The operator $\hat{H}^{02}_{\mathrm{mix}}$ mixes the states of the 0p-0h and 2p-2h configurations while $\hat{H}^{24}_{\mathrm{mix}}$ does the same for the 2p-2h and 4p-4h configurations. This mixing directly follows from the two-body nature of the shell-model interaction.

3. Geometry of the IBM with configuration mixing

The algebraic formalism of the previous section does not directly provide a geometry for the IBM Hamiltonian. A way to establish a connection [13] with the geometric Bohr-Mottelson model [14], is obtained by defining a coherent state with fixed boson number [2]

$$|N, \beta\gamma\rangle \equiv \left(s^\dagger + \beta \left[\cos\gamma d_0^\dagger + \sqrt{\tfrac{1}{2}} \sin\gamma (d_{+2}^\dagger + d_{-2}^\dagger) \right] \right)^N |\mathrm{o}\rangle,$$

which endows the algebraic model with an intrinsic geometric structure in terms of the quadrupole-shape variables β and γ. For each of the separate Hamiltonians $\hat{H}_{i\mathrm{p}-i\mathrm{h}}$ in (2) one obtains from its expectation value in the coherent state an energy surface

$$E_i(\beta,\gamma) = \frac{N_i \epsilon_i \beta^2}{1+\beta^2} + \kappa_i \left[\frac{N_i(5 + (1+\chi_i^2)\beta^2)}{1+\beta^2} + \frac{N_i(N_i-1)}{(1+\beta^2)^2} \left(\frac{2}{7}\chi_i^2 \beta^4 + 4\sqrt{\frac{2}{7}} \chi_i \beta^3 \cos 3\gamma + 4\beta^2 \right) \right], \quad (4)$$

TABLE I. Parameters in the first [10] and second [15] IBM fits of the three coexisting configurations in the Pb isotope chain.

Ref. fit	Configuration	ϵ	κ	χ	Δ	$\omega_0 = \omega_2$
[10]	0p-0h	0.90	0	-	-	-
	2p-2h	0.51	-0.014	0.515	1.880	0.0150
	4p-4h	0.55	-0.020	-0.680	4.000	0.0300
[15]	0p-0h	0.92	0	-	-	-
	2p-2h	0.51	-0.014	0.515	1.923	0.0085
	4p-4h	0.55	-0.020	-0.680	3.846	0.0234

where $N_i = N + i$ is the boson number associated with that particular configuration.

For the lead isotopes in particular ($^{186-208}$Pb), a set of parameters ($\epsilon, \kappa, \chi, \Delta$ and ω) describes a potential energy surface for N ranging from 0 to 11 bosons (for neutron numbers from the closed shell $N = 126$ to mid-shell $N = 104$). The 0p-0h configuration corresponds to N bosons whereas the 2p-2h and 4p-4h excitations require 2 and 4 additional bosons, respectively. This leads to a 3×3 *potential energy matrix* [11]

$$\mathbf{E}_N(\beta,\gamma) = \begin{pmatrix} E_0(\beta,\gamma) & \Omega_{02}(\beta) & 0 \\ \Omega_{02}(\beta) & E_2(\beta,\gamma)+\Delta_2 & \Omega_{24}(\beta) \\ 0 & \Omega_{24}(\beta) & E_4(\beta,\gamma)+\Delta_4 \end{pmatrix}, \quad (5)$$

where Δ_2 (Δ_4) corresponds to the single-particle energy expended in raising 2 (4) protons from the lower (50-82) to the upper (82-126) shell, corrected for the gain in energy due to pairing, and where $\Omega_{ii'}(\beta) \equiv \langle N+i, \beta\gamma|\hat{H}^{ii'}_{\rm mix}|N+i', \beta\gamma\rangle$ are the non-diagonal matrix elements

$$\Omega_{02}(\beta) = \frac{\sqrt{(N+1)(N+2)}}{1+\beta^2}\left(\omega_0^{02} + \omega_2^{02}\beta^2\right),$$

$$\Omega_{24}(\beta) = \frac{\sqrt{(N+3)(N+4)}}{1+\beta^2}\left(\omega_0^{24} + \omega_2^{24}\beta^2\right). \quad (6)$$

The eigenpotentials of the matrix (5) are obtained by diagonalization. The eigensolutions depend on the parameters ϵ_i, κ_i, χ_i, and $\omega_k^{ii'}$ which are taken *without any modification* from a comprehensive fit to the energy spectra of several nuclei in the lead mass region and shown in Table I.

The first set [10] produces results similar to the ones of this paper [11], obtained with a second set of parameters [15]. The major difference between these parameters is that the second has much smaller mixing values (ω), because in the first fit they were oversetimated. The 0p-0h configuration is found to be spherical ($\kappa_0 = 0$) while the 2p-2h and 4p-4h configurations turn out to be oblate ($\kappa_2 \neq 0$, $\chi_2 > 0$) and prolate ($\kappa_4 \neq 0$, $\chi_4 < 0$) in both fits, respectively.

In Fig. 2 the potential energy surfaces in β and γ resulting from $\mathbf{E}_N(\beta,\gamma)$ are shown for the nucleus ^{186}Pb.

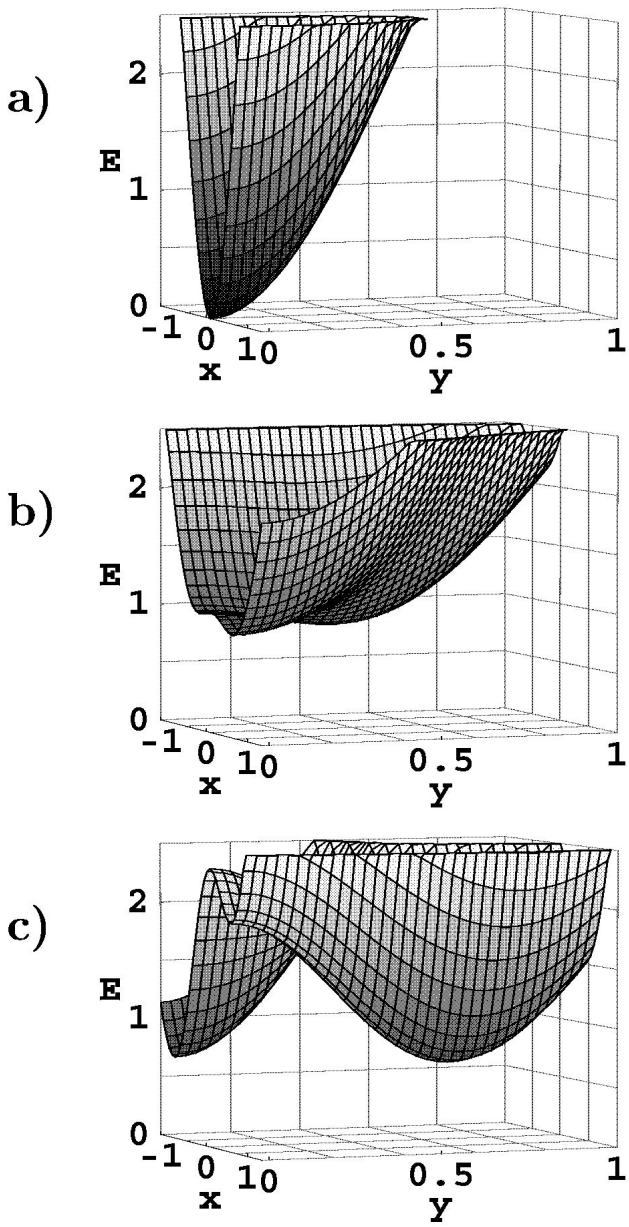

FIGURE 2. Potential energy surfaces in β and γ for ^{186}Pb. On the horizontal axes, x $\equiv \beta\sin(\gamma + 30^o)$ runs from -1 to 1, while y $\equiv \beta\cos(\gamma + 30^o)$ runs from 0 to 1. The vertical axis gives the energy in MeV. The three plots show (a) the 0p-0h configuration before mixing, (b) the 2p-2h configuration before mixing, and (c) the 4p-4h configuration before mixing.

Inserts 2a-c give the separate 0p-0h, 2p-2h, and 4p-4h configurations before mixing. The first of these exhibits a minimum with spherical shape at $\mathrm{a} \equiv \beta \sin(\gamma + 30°) = 0$ and $\mathrm{b} \equiv \beta \cos(\gamma + 30°) = 0$. The 2p-2h configuration (insert b) has an oblate minimum at $\mathrm{a} = -0.21$, $\mathrm{b} = 0.37$ ($\beta = 0.43$, $\gamma = \pm 60°$) with an energy of 820 keV. A prolate minimum occurs for the 4p-4h configuration at $\mathrm{a} = 0.36$, $\mathrm{b} = 0.62$ ($\beta = 0.72$, $\gamma = 0°$) with an energy of 848 keV. These energies are reasonably close to those of the 0^+ excited states observed in ^{186}Pb.

The plots in Fig. 3 show two views of the potential energy surface of the lowest energy eigenvalue of $\mathbf{E}_N(\beta, \gamma)$ in Eq. (5) using the second set of parameters in Table I. The potential energy surface of Fig. 3 exhibits a remarkable similarity with that obtained within a mean-field approach [6] (apart from an overall factor in β). Nevertheless, with the mixing as determined in Ref. 10only two (spherical and prolate) of the three minima remain. There is, however, still considerable uncertainty in the exact value of the mixing. A reduction of the mixing leads to *three* minima in the lowest eigenpotential of (5) which otherwise is very similar in appearance to the surface shown in Fig. 3.

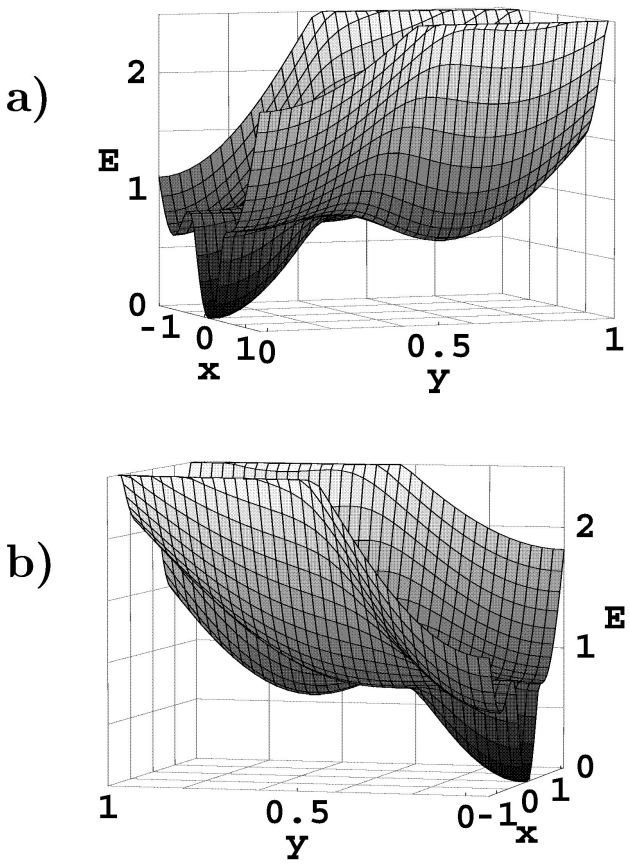

FIGURE 3. Two views of potential energy surfaces for ^{186}Pb after configuration mixing.

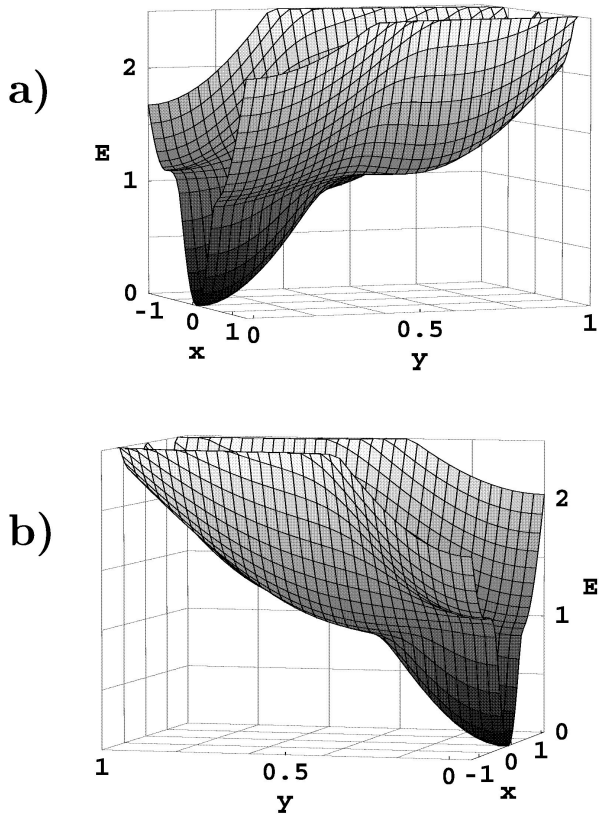

FIGURE 4. Two views of potential energy surfaces for ^{188}Pb after configuration mixing.

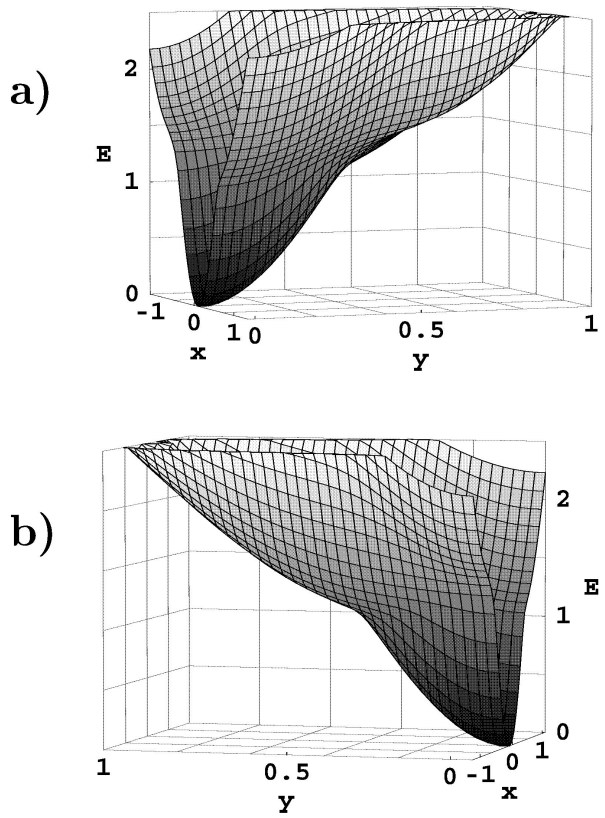

FIGURE 5. Two views of potential energy surfaces for ^{190}Pb after configuration mixing.

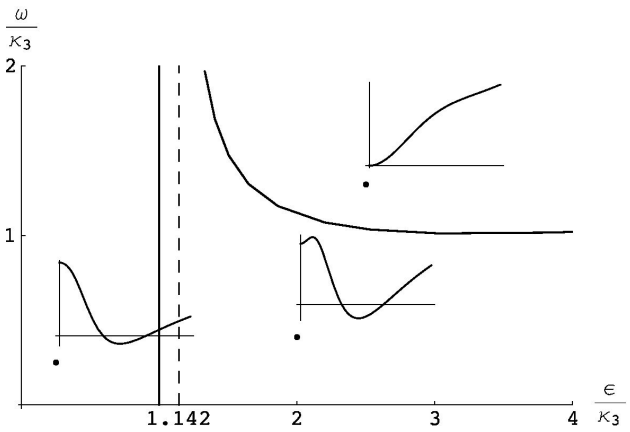

FIGURE 6. Phase diagram for U(5)–SU(3) configuration mixing.

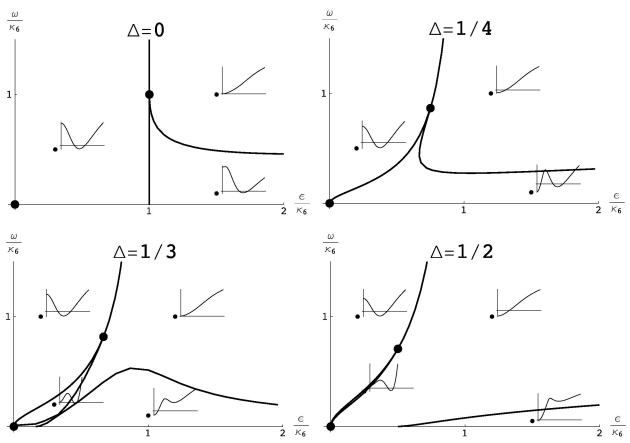

FIGURE 7. Phase diagrams for U(5)–SO(6) configuration mixing. The figures show the physical region of the parameter space with $\bar{\epsilon}/\bar{\kappa}_6 > 0$ and, since the problem is invariant under $\bar{\omega} \to -\bar{\omega}$, only $\bar{\omega}/\bar{\kappa}_6 > 0$ is shown. The figures correspond to $\Delta = 0$, 1/4, 1/3, and 1/2. Different phases are separated by critical lines (thick lines) and three phases meet in triple points (dots). The inset plots illustrate the potential for the different phases.

In Figs. 4 and 5 are shown the potential energy surfaces in ^{188}Pb and ^{190}Pb, respectively. The same point of view and scale were used to make evident the dissapearance of the coexisting minima.

4. Coexistence and criticality

The geometric interpretation of the IBM with configuration mixing may also improve our understanding of the relation between coexistence and criticality. The different phases of the IBM-1 have been rigorously determined on the basis of catastrophe theory [16] and its phase diagram is well established [17]. In particular, it is known [18] that there is little scope for coexistence and only coexistence of spherical and deformed shapes [U(5)-SU(3)]. The present matrix coherent-state formalism broadens the scope of this investigation: A catastrophe analysis, similar to that in Ref. [16], can be undertaken of the IBM with configuration mixing. A first analysis indicates a wealth of new results such as phase diagrams with spherical-deformed and prolate-oblate coexistence, triaxial instabilities as well as a connection with the critical symmetries proposed by Iachello [19].

In the case of the mixing of two consistent-q formalism (CQF) Hamiltonians for N and $N+2$ bosons, respectively, a potential surface in terms of U(5) and SU(3) symmetries, is obtained from the diagonalization of the potential matrix

$$\begin{bmatrix} \bar{\epsilon}\dfrac{\beta^2}{1+\beta^2} & \bar{\omega} \\ \bar{\omega} & -\bar{\kappa}_3\dfrac{\beta^4+4\sqrt{2}\beta^3\cos 3\gamma+8\beta^2}{2(1+\beta^2)^2}+\Delta \end{bmatrix}, \quad (7)$$

where $\bar{\epsilon} = \tilde{N}\epsilon$, $\bar{\kappa}_3 = 4\bar{\kappa} = 4\tilde{N}(\tilde{N}-1)\kappa$, $\tilde{N}$ is either N or $N+2$ and, furthermore, $\bar{\omega}_i = \sqrt{(N+1)(N+2)}\omega_i$ is introduced for notational convenience. We choose $\bar{\kappa}_3 = 1$ and express $\bar{\epsilon}$, $\bar{\omega}$, and Δ in units $\bar{\kappa}_3$.

The criticality conditions in β and γ are given by

$$\frac{\partial E_-}{\partial \beta} = \frac{\partial^2 E_-}{\partial \beta^2} = 0, \quad (8)$$

which is valid for U(5)–SU(3) mixing but not in general.

If $\gamma = 0$, the lowest eigenvalue of (7) can be expanded in β as

$$E_-(\beta, \gamma = 0; \bar{\epsilon}, \bar{\omega}, \Delta = 0) \approx -\bar{\omega} + \frac{\bar{\epsilon}-1}{2}\beta^2 - \frac{1}{\sqrt{8}}\beta^3 + \cdots, \quad (9)$$

which shows that for $\bar{\epsilon} < 1$ the minimum is deformed while for $\bar{\epsilon} > 1$ there is a spherical minimum (see Fig. 6).

Furthermore, for a given deformation $\beta_0 \neq 0$ the conditions for criticality can be solved for $\bar{\epsilon}$ and $\bar{\omega}$, which leads to a parametric representation of the locus of points where the potential changes character from one with a spherical minimum to one with two coexisting minima. In the U(5)–SU(3) case, this critical curve does not meet the line $\bar{\epsilon} = 1$ but converges to the value 1.14168... for $\bar{\omega} \to \infty$. We thus see that the small region of coexistence in the single-configuration U(5) to SU(3) transition ($1 < \bar{\epsilon} < 1.14168\ldots$) is considerably expanded if configuration mixing is allowed.

Increasing Δ shifts the critical line to the left and the region with a deformed minimum shrinks. In Fig. 7 the two critical lines remain separated for all values of Δ: no triple point exists for physical values of the parameters. Finally, as Δ increases, the critical curve with $\beta_0 \neq 0$ moves down in the $\bar{\epsilon}$–$\bar{\omega}$ plane.

Mixing of U(5) and SO(6) leads the potential matrix depending on β only and is given by

$$\begin{bmatrix} \bar{\epsilon}\dfrac{\beta^2}{1+\beta^2} & \bar{\omega} \\ \bar{\omega} & -\bar{\kappa}_6\dfrac{\beta^2}{(1+\beta^2)^2}+\Delta \end{bmatrix}, \quad (10)$$

where $\bar{\kappa}_6 = 4\bar{\kappa}$ is introduced for notational convenience. Since the problem is scale invariant, we may choose $\bar{\kappa}_6 = 1$;

this means that $\bar{\epsilon}$, $\bar{\omega}$, and Δ are expressed in units $\bar{\kappa}_6$. For $\Delta = 0$, the lowest eigenvalue of (10) can be expanded in β as

$$E_-(\beta;\bar{\epsilon},\bar{\omega},\Delta=0) \approx -\bar{\omega} + \frac{\bar{\epsilon}-1}{2}\beta^2 - \frac{(1+\bar{\epsilon})^2 + 4(\bar{\epsilon}-2)\bar{\omega}}{8\bar{\omega}}\beta^4 + \cdots \tag{11}$$

while for $\Delta \neq 0$, the lowest energy eigenvalue is given by

$$E_-(\beta;\bar{\epsilon},\bar{\omega},\Delta) \approx \frac{\Delta}{2}\left(1-\sqrt{1+4\zeta}\right) + \frac{(1+\bar{\epsilon})-(1-\bar{\epsilon})\sqrt{1+4\zeta}}{2\sqrt{1+4\zeta}}\beta^2 - \frac{2\zeta(1+\bar{\epsilon})^2 + \Delta(1+4\zeta)[(2+\bar{\epsilon})-(2-\bar{\epsilon})\sqrt{1+4\zeta}]}{2\Delta(1+4\zeta)^{3/2}}\beta^4 + \cdots, \tag{12}$$

where $\zeta = \bar{\omega}^2/\Delta^2$.

When $\Delta = 0$, the line $\bar{\epsilon} = 1$ is critical in the sense that on its left ($\bar{\epsilon} < 1$) the potential has a deformed minimum while on its right ($\bar{\epsilon} > 1$) it has a spherical one (see Fig. 7). This is similar to what is found for the U(5) to SO(6) transition in the IBM with a single configuration.

The main result is that, unlike in the single-configuration U(5) to SO(6) transition, a region of coexistence is present in the mixing of U(5) and SO(6) configurations. To find the position of the triple point, we require in addition that the coefficient of β^4 vanishes. This leads to the solutions

$$(\bar{\epsilon}_0,\bar{\omega}_0) = (1-\Delta, \pm\sqrt{1-\Delta}) \text{ or } (\bar{\epsilon}_0,\bar{\omega}_0) = (0,0), \tag{13}$$

where $\bar{\epsilon}_0, \bar{\omega}_0$ are the control parameters when we choose β_0.

When Δ increases, the triple point migrates downwards to the left and reaches (0,0) for $\Delta = 1$. Before that, at values of $\Delta > 1/4$, a spherical region appears in the physical phase diagram around $(\bar{\epsilon},\bar{\omega}) = (0,0)$. The two spherical regions touch at $\Delta \approx 1/3$, point at which the region of coexisting minima splits into two. One of these regions shrinks rapidly and disappears altogether for $\Delta = 1$; the other region of coexisting minima never disappears but shifts to higher values of $\bar{\epsilon}$ as Δ increases.

A catastrophe analysis is the subject of a separate paper [20].

5. Conclusion

The main aim of this paper is to give a geometric interpretation of the IBM with configuration mixing via a matrix coherent-state method. The application to the lead isotopes and the similarities found between the mean-field approach and the geometric interpretation of the IBM, suggest that this geometric interpretation is a reliable tool in the description of shape coexistence phenomena in nuclei. The lowest potential energy surface predicted with matrix coherent states is in agreement with that found using mean-field theory while it is at the same time derived from an IBM Hamiltonian that describes the known spectroscopic properties of the lead isotopes.

The proposed matrix coherent-state method opens up the possibility for a systematic investigation of the relation between coexistence and criticality. In contrast to IBM-1, where coexistence plays a marginal role only and where it is confined to a small U(5)-SU(3) region, coexistence acquires a prominent status in the IBM with configuration mixing and can be studied in full detail by applying a catastrophe theory of critical behaviour to the eigenpotentials obtained from the matrix coherent-state method. The structure of the phase diagram is rather complex, which can be traced back to the non-polinomial character of the eigenpotential in terms of β.

Acknowledgments

This work was supported in part by CONACyT (Mexico).

1. K. Heyde, P. Van Isacker, M. Waroquier, J.L. Wood, and R.A. Meyer, *Phys. Rep.* **102** (1983) 293; J.L. Wood, K. Heyde, W. Nazarewicz, M. Huyse, and P. Van Duppen, *Phys. Rep.* **215** (1992) 101.
2. R. Gilmore, *J. Math. Phys.* **20** (1979) 891.
3. P. Federman and S. Pittel, *Phys. Lett. B* **69** (1977) 385.
4. F.R. May, V.V. Pashkevich, and S. Frauendorf, *Phys. Lett. B* **68** (1977) 113.
5. W. Nazarewicz, *Phys. Lett. B* **305** (1993) 195.
6. A.N. Andreyev *et al.*, *Nature* **405** (2000) 430.
7. T. Duguet, M. Bender, P. Bonche, and P.-H. Heenen, *Phys. Lett. B* **559** (2003) 201.
8. F. Iachello and A. Arima, *The Interacting Boson Model*, (Cambridge University Press, Cambridge, 1987).
9. P.D. Duval and B.R. Barrett, *Nucl. Phys. A* **376** (1982) 213.

10. R. Fossion, K. Heyde, G. Thiamova, and P. Van Isacker, *Phys. Rev. C* **67** (2003) 024306.
11. A. Frank, P. Van Isacker, and C.E. Vargas, *Phys. Rev. C* **69** (2004) 034323.
12. D.D. Warner and R.F. Casten, *Phys. Rev. C* **28** (1983) 1798; P.O. Lipas, P. Toivonen, and D.D. Warner, *Phys. Lett. B* **155** (1985) 295.
13. J.N. Ginocchio and M.W. Kirson, *Phys. Rev. Lett.* **44**,(1980) 1744; A.E.L. Dieperink, O. Scholten, and F. Iachello, *Phys. Rev. Lett.* **44** (1980) 1747; A. Bohr and B.R. Mottelson, *Phys. Scripta* **22** (1980) 468.
14. A. Bohr and B.R. Mottelson, *Nuclear Structure. II Nuclear Deformations* (Benjamin, New York, 1975).
15. R. Fossion and K. Heyde, Private communications.
16. E. López-Moreno and O. Castaños, *Phys. Rev. C* **54** (1996) 2374.
17. J. Jolie, R.F. Casten, P. von Brentano, and V. Werner, *Phys. Rev. Lett.* **87** (2001) 162501.
18. F. Iachello, N.V. Zamfir, and R.F. Casten, *Phys. Rev. Lett.* **81** (1998) 1191.
19. F. Iachello, *Phys. Rev. Lett.* **85** (2000) 3580; *ibid.* **87** (2001) 052502; *ibid.* **91** (2003) 132502.
20. P. Van Isacker, A. Frank, and F. Iachello, submitted for publication.